Letter

Gold Nanoparticles-Induced Photocurrent Quenching and Recovery of Polymer Dots: Toward Signal-On Energy-Transfer-Based Photocathodic Bioanalysis of Telomerase Activity in Cell Extracts

Ling Zhang, Xiao-Mei Shi, Yi-Tong Xu, Gao-Chao Fan,
Yan Yu Liang, Chengshuang Wang, and Wei-Wei Zhao

Anal. Chem., **Just Accepted Manuscript** • DOI: 10.1021/acs.analchem.8b05370 • Publication Date (Web): 07 May 2019

Gold Nanoparticles-Induced Photocurrent Quenching and Recovery of Polymer Dots: Toward Signal-On Energy-Transfer-Based Photocathodic Bioanalysis of Telomerase Activity in Cell Extracts

Ling Zhang,[1,2] Xiao-Mei Shi,[2] Yi-Tong Xu,[2] Gao-Chao Fan,[3] Yan-Yu Liang,[1,*] Chengshuang Wang,[4,*] Wei-Wei Zhao[2,*]

[1]School of Materials Science and Technology, Nanjing University of Aeronautics and Astronautics, Nanjing 211106, China

[2]State Key Laboratory of Analytical Chemistry for Life Science, School of Chemistry and Chemical Engineering, Nanjing University, Nanjing 210023, China

[3]Shandong Key Laboratory of Biochemical Analysis, College of Chemistry and Molecular Engineering, Qingdao University of Science and Technology, Qingdao 266042, China.

[4]Department of Chemical and Environmental Engineering, University of California, Riverside. Riverside, California 92521, United States

* To whom correspondence should be addressed.

*E-mail: liangyy403@126.com

*E-mail: cwang@ucr.edu

*E-mail: zww@nju.edu.cn

ABSTRACT: Energy transfer (ET) in photoelectrochemical (PEC) bioanalysis was usually generated between noble metal nanoparticles (NPs) and traditional inorganic quantum dots (QDs). Using the innovative polymer dots (Pdots)-involved ET, this work reports the first signal-on and cathodic PEC bioanalysis toward telomerase (TE) activity in cell extracts. Specifically, the sequential binding of capture DNA (cDNA), telomerase primer sequence (TS) and Au NPs-labeled probe DNA (Au NPs-pDNA) on the electrode would place the Au NPs in close proximity of Pdots, leading to obvious quenching of the cathodic photocurrent. The subsequent extension of the TS by TE in the presence of deoxyribonucleoside triphosphates (dNTPs) would then release the Ag NPs-pDNA from the electrode, leading to the recovery of the photocurrent. On the basis of the Au NPs-induced photocurrent quenching and recovery of Pdots, a sensitive biosensor could thus be developed by tracking the photocurrents to probe the TE activity. This strategy allows for signal-on and cathodic PEC bioanalysis of TE, which can be easily extended for numerous other targets of interest. We believe this work could offer a new perspective for the rational implementation of Pdots-involved ET for advanced PEC bioanalysis.

KEYWORDS: Photoelectrochemical bioanalysis; Signal on; Energy transfer; Polymer dots; Gold nanoparticles; Telomerase activity

As a ribonucleoprotein enzyme transcriptase, human telomerase (TE) can induce the addition of repeated sequences $(TTAGGG)_n$ onto the 3' end of telomeres, and facilitate the infinite cellular proliferation.[1-3] It is widely confirmed that TE in 85% of cancer cell is over-expressed, which makes TE to be regarded as a credible biomarker for the early diagnosis and treatment of cancers.[4,5] Therefore, the detection of TE activity has attracted more attention in recent years.[6,7] Previous techniques established for TE activity detection include the fluorescent, colorimetric and traditional electrochemical techniques. While every strategy has distinct advantages, each also has its own drawbacks such as poor sensitivity and laborious procedures. Therefore, accurate and ultrasensitive TE activity detection is still highly appealing. As a rapidly developing bioanalytical technique, photoelectrochemical (PEC) offers an exquisite route to probe various specific biological events.[8,9] However, due to the short development time, the novel signaling mechanisms still need to be exploited.

Energy transfer (ET) phenomena in PEC systems have initially been observed between noble metal NPs and traditional inorganic CdS quantum dots (QDs),[10,11] which rapidly catalyzed increasing ET-based PEC bioanalytical studies.[12-20] Specifically, the exciton states of CdS QDs can be modulated owing to the ET from the adjacent noble metal NPs, which ultimately resulted in the quenching of PEC signal. Despite previous progress, these reports almost focused on various inorganic QDs-based systems. Polymer dots (Pdots) represent a promising family of functional nanomaterials with excellent chemical, electrical and optical properties.[12] Compared with traditional QDs, Pdots have many attractive features such as low cytotoxicity, facile functionalization, and high biocompatibility.[21-23] Recently, we further verified the existence of ET between Au NPs and semiconducting Pdots and then tested it for signal-off PEC DNA bioanalysis.[24] Despite this preliminary study, the exploitation in this emerging direction is in its very infancy. On the other hand, compared with common signal-off and anodic protocols[25-28], signal-on[6, 29-30] and cathodic[31-35] ones are more actively pursued in current PEC bioanalysis.

Herein we report the realization of signal-on and cathodic PEC bioanalysis of TE activity in cell extracts, on the basis of the gold nanoparticles (Au NPs)-induced

ET-based photocurrent quenching and recovery of Pdots. Specifically, as shown in Scheme 1, the system operated upon the sequential binding of capture DNA (cDNA), telomerase primer sequence (TS) and Au NPs-labeled probe DNA (Au NPs-pDNA) on the poly[(9,9-dioctylfluorenyl-2,7-diyl)-co-(1,4-benzo-thiadazole)] (PFBT) Pdots/indium tin oxide (ITO) electrode, which was followed by the subsequent extension of the TS by the TE in the presence of deoxyribonucleoside triphosphates (dNTPs) and thereby the release of Au NPs-pDNA from the electrode (See Supporting Information for DNA sequences and Experimental Section). Upon the presence and absence of Au NPs-pDNA, the cathodic photocurrent of PFBT Pdots/ITO electrode would be efficiently quenched and recovered, respectively, and thereby a sensitive photocathodic biosensor could be tailored by tracking the photocurrent to probing the TE activity. Based on the Pdots/ITO electrode, this work realized the first signal-on ET-based photocathodic bioanalysis which to our knowledge has not been reported. We believe it will generate more interest in the exploration of Pdots-involved ET phenomena for advanced signal-on cathodic PEC bioanalysis.

Scheme 1. Signal-On ET-Based Photocathodic Bioanalysis of TE Activity in Cell Extracts

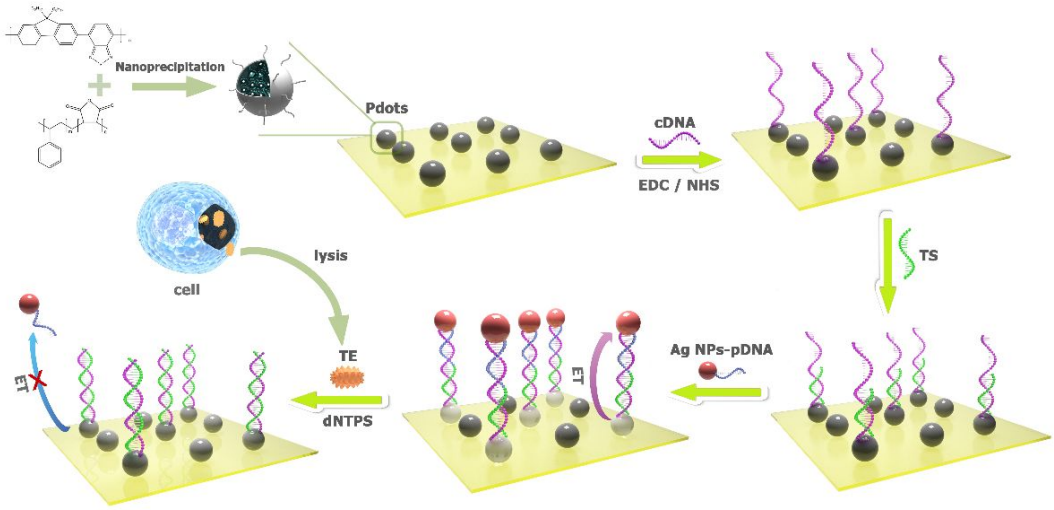

RESULTS AND DISCUSSION

Characterization. In this work, Pdots were prepared through reprecipitation method[36] using conjugated PFBT polymer and functional polymer poly styrene-co-maleic anhydride (PSMA). As shown in Figure 1a, the high-resolution transmission electron microscope (HR-TEM) image implies that the as-obtained PFBT Pdots possess quasi-spherical shape of an average particle diameter of ca. 5 nm. The corresponding Fourier-transform infrared (FTIR) spectrum in Figure 1b demonstrates the successful functionalization of carboxyl groups on the Pdots surface. Specifically, the wide and strong absorption bands around 3000 cm^{-1} were ascribed to the coupling effects of stretching vibration of O-H in carboxyl groups and C-H bonds. Meanwhile, the absorption peak at 1715 cm^{-1} attributed to the stretching vibration of C=O further demonstrated the successful functionalization of carboxyl groups on the sample. Figure 1c inset reveals the synthetic Au NPs also have a similar size corresponding to ca. 5 nm with uniform distribution. And the optical characterization of the prepared PFBT Pdots and Au NPs is illustrated in Figure 1c. The black curve indicated that the PFBT Pdots had a broad-band absorption in the visible range of 400-550 nm, which implied its potential as photoactive species for the construction of PEC bioanalysis platform. The emission spectrum of the proposed PFBT Pdots (blue curve in figure 1c) presents its fluorescence ranged from 500 to 700 nm with the emission peak at ca.544 nm. Meanwhile, as the red curve shown, the absorption spectrum of Au NPs is clearly characterized by the maximum absorption at 515 nm. Obviously, this characteristic plasmon absorption of Au NPs has a partial overlap with the broad emission range of PFBT Pdots, which makes the energy transfer process possible between the two nanoparticles. Followed by functionalization with probe DNA (pDNA) via the Au-S bonding, the surface charges of Au NPs would be changed which results in the maximum absorption of Au NPs in the UV-vis absorption spectra slight red shifting to around 523 nm, as shown in Figure 1d. Meanwhile, a new characteristic peak of nucleic acids at ca. 256 nm appeared, giving evidence of the successful coupling of the pDNA on Au NPs. In addition, as shown in Figure 1d inset, the prepared Au NPs-pDNA had more negative zeta potential than Au NPs, which further confirmed the pDNA functionalization Au NPs had been

synthesized.

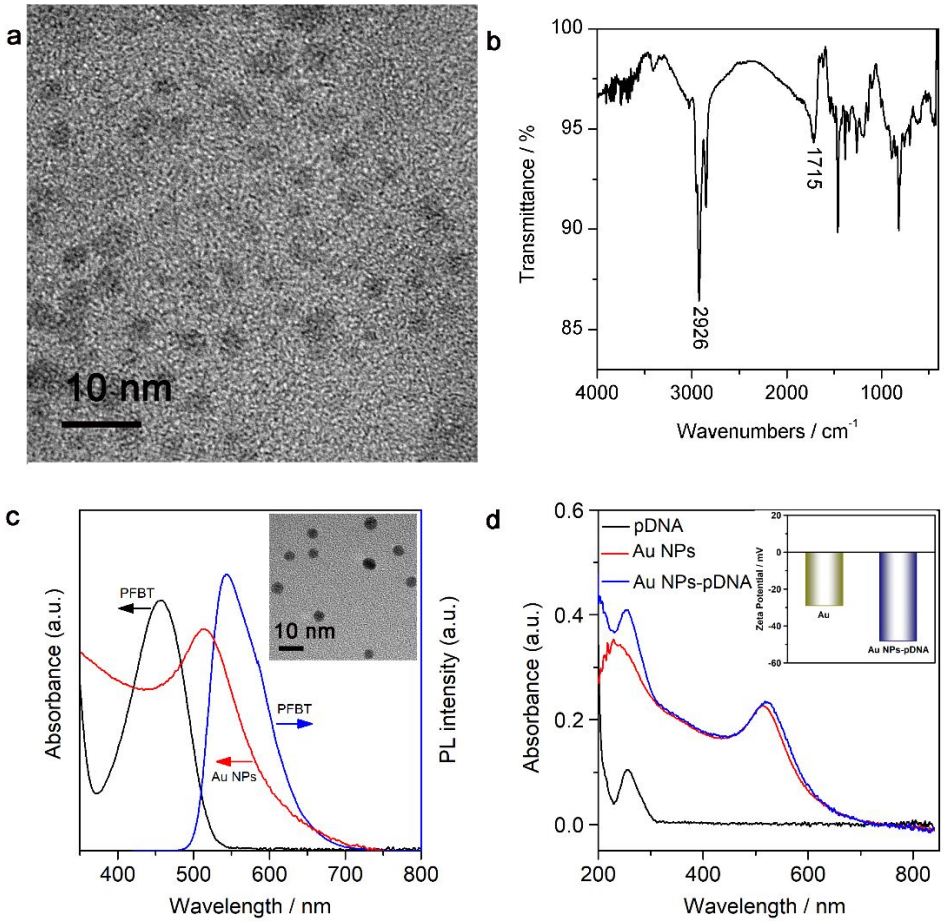

Figure 1. (a) TEM image of the fabricated PFBT Pdots. (b) FTIR spectra of the PFBT Pdots. (c) UV-vis absorption spectra of PFBT Pdots and Au NPs and emission spectra of the PFBT Pdots under the excitation wavelength at 450 nm. Inset: TEM image of the synthetic Au NPs. (d) UV-vis absorption spectra of pDNA, Au NPs and Au NPs-pDNA. Inset: Zeta potentials of Au NPs and Au NPs-pDNA in H_2O.

Feasibility. To study the feasibility, polyacrylamide gel electrophoresis (PAGE) is employed firstly. As shown in Figure 2a, lanes 1, 2, 3 and 4 are observed for 20 bp marker, pDNA, TS and cDNA, respectively. When pDNA is incubated with TS and cDNA at 37 ℃ for 2 h, a new band (lane 5) with larger molecular weight would appear, indicating the formation of a DNA complex. Followed by the addition of TE extraction and dNTPs and incubation at 37 ℃ for another 2 h, the land of pDNA (lane 2) appears in lane 6, demonstrating the anchored pDNA has been displaced

successfully due to the elongation of TS.

The system is then directed for the PEC study on a PFBT Pdots/ITO electrode. Figure S1 shows the optimization of Pdots layers on ITO, and Figure S2 then records the corresponding photocurrent intensity upon different biases voltage. Obviously, the observed cathodic photocurrent is sensitive to the electron acceptor of dissolved oxygen (O_2), which was confirmed by the deoxygenation tests in Figure S3. Besides, Figure S4 and S5 illustrated the operational stability of the electrode. Following the optimization of the incubation time of TS and Ag NPs-pDNA as shown in Figure S6, the above-mentioned reaction processes are carried out on the Pdots/ITO electrode and the corresponding photocurrent signals are recorded. As demonstrated in Figure 2b, under the intermittent light excitation at 450 nm, the Pdots/ITO electrode exhibits a cathodic photocurrent about 95 nA (curve a). After the immobilization of cDNA and the blocking by monoethanolamine (MEA), the photocurrent decreases about 22 % (curve b), which might be ascribed to the anchoring layer inhibiting the electron transfer. Hybridization with TS induces further reduction of signal intensity (curve c). After conjugated with Au NPs-pDNA, the photocurrent intensity of Pdots presents sharp decrease (curve d). This is because that the local electric fields originated from plasmon resonance of the Au NPs could modulate the exciton states in photoactivated Pdots via ET, leading to the quenching of the photocurrent signal of Pdots electrode. [10,11] However, the addition of TE extract and dNTPs results in an obvious increase in photocurrent intensity (curve e). This is because that the extension of the TS would release the Au NPs-pDNA from the electrode and thus remove the ET influence against the Pdots electrode, leading to the recovery of the signal. The changes in the photocurrent intensity during the detection of 600 Hela cells have also been presented in Figure S7. In addition, the quenching and recovery steps are further proofed though the fluorescence images of electrode during the reaction processes (Figure S8). Furthermore, the corresponding cyclic voltammograms (CV) and the electrochemical impedance spectroscopy (EIS) had also been performed as shown in Figure S9 and S10, respectively.

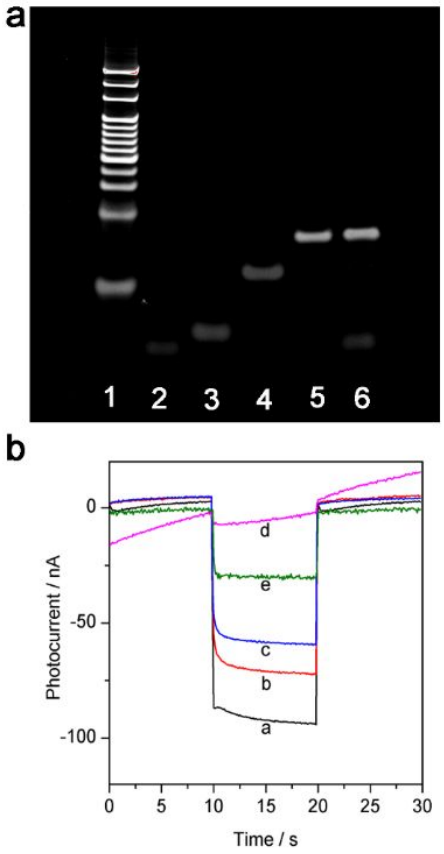

Figure 2. (a) Electrophoresis image of DNA ladder (lane 1), pDNA (lane 2), TS (lane 3), cDNA (lane 4), the mixture of pDNA, TS and cDNA (lane 5), the mixture of pDNA, TS and cDNA after the addition of dNTPs and cell extraction (lane 6). (b) The photocurrent responses of the proposed PFBT Pdots/ITO electrode before (curve a) and after modification with cDNA and MEA (curve b), TS (curve c), Au NPs-pDNA (curve d) and the mixture of 2.5 mM dNTPs and cell extration of 8000 HeLa cells (curve e).

Performance. By incubation with different concentration of TE in the presence of dNTPs at 37℃ for 2 h, the performance of the proposed signal-on photocathodic enzymatic bioanalysis was studied. As shown in Figure 3a, with the number of HeLa cells raised from 30 to 20000 in the 20 μL reaction mixture, more Au NPs-DNA would be displaced from the electrode due to the TE-triggered elongation of TS and the corresponding photocurrent intensity would be enhanced to different extent. The detection limit was found experimentally to be of 30 Hela cells, which is comparable to some recent TE biosensors, as listed in Table S2. Figure 3a inset presents that the increase of the cathodic photocurrent is proportional to the number of cells with the linear range from 100 to 800 and 2000 to 16000, respectively. And Figure S11

demonstrated the photocurrent responses of the modified Pdots electrodes to TE activity in different numbers of HeLa cells extracts. The relative standard deviation (RSD) is calculated to be 6.3% though testing 600 HeLa cells with five TE-triggered probes prepared at the same conditions, indicating the proposed signal-on PEC enzymatic bioanalysis has satisfactory reproducibility. The specificity of the protocol is demonstrated by detecting the cell extraction of HeLa cells, heated-HeLa cells, and coexisting interfering substances in the cell extract such as dopamine (DA), glutathione (GSH), ascorbic acid (AA) and lysozyme (LZM). The results in Figure 3b shows that these interfering species almost have no obvious influence compared to that of TE, which reveals the reliable selectivity of the protocol. Furthermore, as shown in Figure S12, the responses of the system against other cancer cells and normal cells have also been detected.

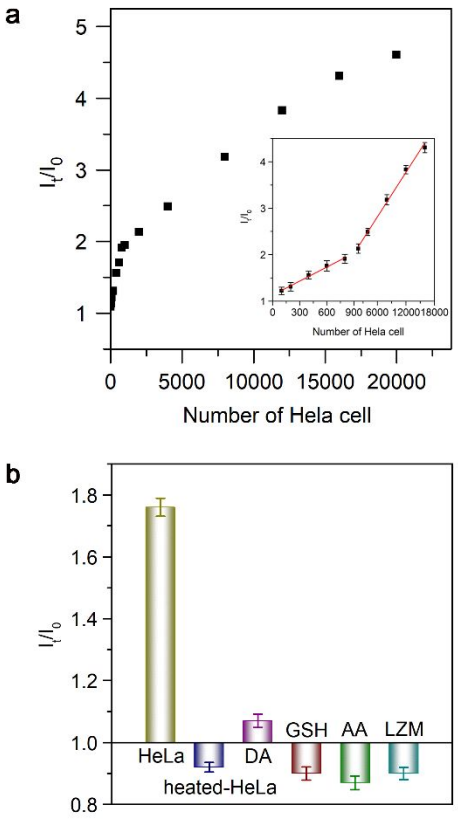

Figure 3. (a) Photocurrent intensity of the electrode corresponding to different number of HeLa cells. Inset: the calibration curves in the ranges from 100 to 800 cells and 2000 to 16000 cells. (b) The specificity of the proposed sensor against HeLa cells and heated-HeLa cells (600 cells), dopamine (DA) (0.2 mM), glutathione (GSH) (0.2 mM), ascorbic acid (AA) (0.2 mM), lysozyme

(LZM) (5 u/g). I_0 and I_t are the photocurrents of the Au NPs-pDNA/TS/cDNA/PFBT Pdots/ITO electrodes prior and after incubated with the mixture of dNTPs and TE or other coexisting interfering substances in the cell extract.

CONCLUSION

Using ET between Au NPs and Pdots, signal-on and cathodic PEC bioanalysis has been successfully realized for probing TE activity in cell extracts. In such a system, the confinement and subsequent release of Au NPs-pDNA from the Pdots electrode would cause obvious photocurrent quenching and recovery, the process of which could be utilized to monitor the biocatalytic event. Experimentally, Pdots and Au NPs are fabricated and characterized. PAGE analysis, PEC measurements and fluorescence imaging are then used to validate the proposed reaction mechanism and the signal variation. In short, such a signal-on and cathodic PEC bioanalysis has not been reported, and the resulting TE activity analysis also exhibited a good performance. This work reveals the potential of Pdots-involved ET for novel PEC bioanalysis, which will make it a useful addition to the armory of advanced ET-based signal-on cathodic PEC bioanalysis in the future.

ASSOCIATED CONTENT

Supporting Information

Chemicals and apparatus, synthesis of Pdots and Au NPs-pDNA, fabrication of Pdots/ITO electrodes, cell culture and the extraction of TE, PEC measurements, biosensor development, experimental optimizations, PEC characterization of the Pdots/ITO electrode, fluorescence images, CV and EIS characterization of the biosensor development process, the comparison of the analytical performance, the responses of the proposed sensor to different cancer cells and normal cells are supplied in this Supporting Information. (PDF)

AUTHOR INFORMATION

Corresponding Authors

*E-mail: liangyy403@126.com

*E-mail: cwang@ucr.edu

*E-mail: zww@nju.edu.cn

ORCID

Yan-Yu Liang: 0000-0003-0151-0742

Wei-Wei Zhao: 0000-0002-8179-4775

Notes

The authors declare no competing financial interest.

ACKNOWLEDGMENTS

We thank the National Natural Science Foundation of China (Grant Nos. 21675080 and 21771107), Natural Science Foundation of Jiangsu Province (Grant Nos. BK20161484 and BK20170073), and the Fundamental Research Funds for the Central Universities (Grant No. NE2015003).

REFERENCES

(1) Blasco, M. A. Telomere length, stem cells and aging. *Nat. Chem. Biol.* **2007,** *3,* 640-649.

(2) Niazov, T.; Pavlov, V.; Xiao, Y.; Gill, R.; Willner, I. DNAzyme-functionalized Au nanoparticles for the amplified detection of DNA or telomerase activity. *Nano Lett.* **2004,** *4,* 1683-1687.

(3) Cohen, S. B.; Graham, M. E.; Lovrecz, G. O.; Bache, N.; Robinson, P. J.; Reddel, R. R. Protein composition of catalytically active human telomerase from immortal cells. *Science* **2007,** *315,* 1850-1853.

(4) Zheng, G.; Daniel, W. L.; Mirkin, C. A. A new approach to amplified telomerase detection with polyvalent oligonucleotide nanoparticle conjugates. *J. Am. Chem. Soc.* **2008,** *130,* 9644-9645.

(5) Herbert, B.-S.; Hochreiter, A. E.; Wright, W. E.; Shay, J. W. Nonradioactive detection of telomerase activity using the telomeric repeat amplification protocol. *Nat. Protoc.* **2006,** *1,* 1583-1590.

(6) Liu, S.; Zhao, S.; Tu, W.; Wang, X.; Wang, X.; Bao, J.; Wang, Y.; Han, M.; Dai, Z. A "Signal On" Photoelectrochemical Biosensor Based on Bismuth@N,O-Codoped-Carbon Core-Shell Nanohybrids for Ultrasensitive Detection

of Telomerase in HeLa Cells. *Chem.-Eur. J.* **2018,** *24,* 3677-3682.

(7) Zavari-Nematabad, A.; Alizadeh-Ghodsi, M.; Hamishehkar, H.; Alipour, E.; Pilehvar-Soltanahmadi, Y.; Zarghami, N. Development of quantum-dot-encapsulated liposome-based optical nanobiosensor for detection of telomerase activity without target amplification. *Anal. Bioanal.Chem.* **2017,** *409,* 1301-1310.

(8) Zhao, W.-W.; Xu, J.-J.; Chen, H.-Y. Photoelectrochemical bioanalysis: the state of the art. *Chem. Soc. Rev.* **2015,** *44,* 729-741.

(9) Kang, Q.; Yang, L.; Chen, Y.; Luo, S.; Wen, L.; Cai, Q.; Yao, S. Photoelectrochemical detection of pentachlorophenol with a Multiple Hybrid CdSexTe1-x/TiO2 Nanotube Structure-Based Label-Free Immunosensor. *Anal. Chem.* **2010,** *82,* 9749-9754.

(10) Zhao, W.-W.; Wang, J.; Xu, J.-J.; Chen, H.-Y. Energy transfer between CdS quantum dots and Au nanoparticles in photoelectrochemical detection. *Chem. Commun.* **2011,** *47,* 10990-10992.

(11) Zhao, W.-W.; Yu, P.-P.; Shan, Y.; Wang, J.; Xu, J.-J.; Chen, H.-Y. Exciton-Plasmon Interactions between CdS Quantum Dots and Ag Nanoparticles in Photoelectrochemical System and Its Biosensing Application. *Anal. Chem.* **2012,** *84,* 5892-5897.

(12) Cai, G.; Yu, Z.; Ren, R.; Tang, D. Exciton Plasmon Interaction between AuNPs/Graphene Nanohybrids and CdS Quantum Dots/TiO2 for Photoelectrochemical Aptasensing of Prostate-Specific Antigen. *ACS Sensors* **2018,** *3,* 632-639.

(13) Dong, Y.-X.; Cao, J.-T.; Wang, B.; Ma, S.-H.; Liu, Y.-M. Exciton-Plasmon Interactions between CdS@g-C3N4 Heterojunction and Au@Ag Nanoparticles Coupled with DNAase-Triggered Signal Amplification: Toward Highly Sensitive Photoelectrochemical Bioanalysis of MicroRNA. *ACS Sustain. Chem. Eng.* **2017,** *5,* 10840-10848.

(14) Fan, G.-C.; Zhu, H.; Shen, Q.; Han, L.; Zhao, M.; Zhang, J.-R.; Zhu, J.-J. Enhanced photoelectrochemical aptasensing platform based on exciton energy transfer between CdSeTe alloyed quantum dots and SiO2@Au nanocomposites.

Chem. Commun. **2015,** *51,* 7023-7026.

(15) Golub, E.; Niazov, A.; Freeman, R.; Zatsepin, M.; Willner, I. Photoelectrochemical Biosensors Without External Irradiation: Probing Enzyme Activities and DNA Sensing Using Hemin/G-Quadruplex-Stimulated Chemiluminescence Resonance Energy Transfer (CRET) Generation of Photocurrents. *J. Phys. Chem. C* **2012,** *116,* 13827-13834.

(16) Ma, Z.-Y.; Ruan, Y.-F.; Xu, F.; Zhao, W.-W.; Xu, J.-J.; Chen, H.-Y. Protein Binding Bends the Gold Nanoparticle Capped DNA Sequence: Toward Novel Energy-Transfer-Based Photoelectrochemical Protein Detection. *Anal. Chem.* **2016,** *88,* 3864-3871.

(17) Tan, Y.; Wang, Y.; Li, M.; Ye, X.; Wu, T.; Li, C. Enhanced photoelectrochemical immunosensing of cardiac troponin I based on energy transfer between N-acetyl-L-cysteine capped CdAgTe quantum dots and dodecahedral Au nanoparticles. *Biosens. Bioelectron.* **2017,** *91,* 741-746.

(18) Zeng, X.; Ma, S.; Bao, J.; Tu, W.; Dai, Z. Using Graphene-Based Plasmonic Nanocomposites to Quench Energy from Quantum Dots for Signal-On Photoelectrochemical Aptasensing. *Anal. Chem.* **2013,** *85,* 11720-11724.

(19) Zhang, L.; Sun, Y.; Liang, Y. Y.; He, J. P.; Zhao, W. W.; Xu, J. J.; Chen, H. Y. Ag nanoclusters could efficiently quench the photoresponse of CdS quantum dots for novel energy transfer-based photoelectrochemical bioanalysis. *Biosens. Bioelectron.* **2016,** *85,* 930-934.

(20) Zhang, Y.; Sun, G.; Yang, H.; Yu, J.; Yan, M.; Song, X. Multifunctional reduced graphene oxide trigged chemiluminescence resonance energy transfer: Novel signal amplification strategy for photoelectrochemical immunoassay of squamous cell carcinoma antigen. *Biosens. Bioelectron.* **2016,** *79,* 55-62.

(21) Wang, L.; Fernandez-Teran, R.; Zhang, L.; Fernandes, D. L. A.; Tian, L.; Chen, H.; Tian, H. Organic Polymer Dots as Photocatalysts for Visible Light-Driven Hydrogen Generation. *Angew. Chem., Int. Ed.* **2016,** *55,* 12306-12310.

(22) Wu, C.; Chiu, D. T. Highly Fluorescent Semiconducting Polymer Dots for Biology and Medicine. *Angew. Chem., Int. Ed.* **2013,** *52,* 3086-3109.

(23) Liu, H.-Y.; Wu, P.-J.; Kuo, S.-Y.; Chen, C.-P.; Chang, E.-H.; Wu, C.-Y.; Chant, Y.-H. Quinoxaline-Based Polymer Dots with Ultrabright Red to Near-Infrared Fluorescence for In Vivo Biological Imaging. *J. Am. Chem. Soc.* **2015,** *137,* 10420-10429.

(24) Shi, X.-M.; Mei, L.-P.; Wang, Q.; Zhao, W.-W.; Xu, J.-J.; Chen, H.-Y. Energy Transfer between Semiconducting Polymer Dots and Gold Nanoparticles in a Photoelectrochemical System: A Case Application for Cathodic Bioanalysis. *Anal. Chem.* **2018,** *90,* 4277-4281.

(25) Jiang, D.; Du, X.; Zhou, L.; Li, H.; Wang, K. New Insights toward Efficient Charge-Separation Mechanism for High-Performance Photoelectrochemical Aptasensing: Enhanced Charge-Carrier Lifetime via Coupling Ultrathin MoS2 Nanoplates with Nitrogen-Doped Graphene Quantum Dots. *Anal. Chem.* **2017,** *89,* 4525-4531.

(26) Li, H.; Mu, Y.; Yan, J.; Cui, D.; Ou, W.; Wan, Y.; Liu, S. Label-Free Photoelectrochemical Immunosensor for Neutrophil Gelatinase-Associated Lipocalin Based on the Use of Nanobodies. *Anal. Chem.* **2015,** *87,* 2007-2015.

(27) Li, M.-J.; Zheng, Y.-N.; Liang, W.-B.; Yuan, R.; Chai, Y.-Q. Using p-type PbS Quantum Dots to Quench Photocurrent of Fullerene-Au NP@MoS2 Composite Structure for Ultrasensitive Photoelectrochemical Detection of ATP. *ACS Appl. Mat. Interfaces* **2017,** *9,* 42111-42120.

(28) Zhang, K.; Lv, S.; Lin, Z.; Li, M.; Tang, D. Bio-bar-code-based photoelectrochemical immunoassay for sensitive detection of prostate-specific antigen using rolling circle amplification and enzymatic biocatalytic precipitation. *Biosens. Bioelectron.* **2018,** *101,* 159-166.

(29) Li, X.; Wang, X.; Zhang, L.; Gong, J. High-Throughput Signal-On Photoelectrochemical Immunoassay of Lysozyme Based on Hole-Trapping Triggered by Disintegrating Bioconjugates of Dopamine-Grafted Silica Nanospheres. *ACS Sensors* **2018,** *3,* 1480-1488.

(30) Shu, J.; Qiu, Z.; Lin, Z.; Cai, G.; Yang, H.; Tang, D. Semiautomated Support Photoelectrochemical Immunosensing Platform for Portable and High-Throughput

Immunoassay Based on Au Nanocrystal Decorated Specific Crystal Facets BiVO4 Photoanode. *Anal. Chem.* **2016,** *88,* 12539-12546.

(31) Li, C.; Lu, W.; Zhu, M.; Tang, B. Development of Visible-Light Induced Photoelectrochemical Platform Based on Cyclometalated Iridium(111) Complex for Bioanalysis. *Anal. Chem.* **2017,** *89,* 11098-11106.

(32) Wang, H.; Zhang, B.; Zhao, F.; Zeng, B. One-Pot Synthesis of N-Graphene Quantum Dot-Functionalized I-BiOCl Z-Scheme Cathodic Materials for "Signal-Off" Photoelectrochemical Sensing of Chlorpyrifos. *ACS Appl. Mat. Interfaces* **2018,** *10,* 35281-35288.

(33) Yan, K.; Liu, Y.; Yang, Y.; Zhang, J. A Cathodic "Signal-off" Photoelectrochemical Aptasensor for Ultrasensitive and Selective Detection of Oxytetracycline. *Anal. Chem.* **2015,** *87,* 12215-12220.

(34) Zheng, Y.-N.; Liang, W.-B.; Xiong, C.-Y.; Yuan, Y.-L.; Chai, Y.-Q.; Yuan, R. Self-Enhanced Ultrasensitive Photoelectrochemical Biosensor Based on Nanocapsule Packaging Both Donor-Acceptor-Type Photoactive Material and Its Sensitizer. *Anal. Chem.* **2016,** *88,* 8698-8705.

(35) Wang, G.-L.; Liu, K.-L.; Dong, Y.-M.; Wu, X.-M.; Li, Z.-J.; Zhang, C. A new approach to light up the application of semiconductor nanomaterials for photoelectrochemical biosensors: Using self-operating photocathode as a highly selective enzyme sensor. *Biosens. Bioelectron.* **2014,** *62,* 66-72.

(36) Wu, C. F.; Szymanski, C.; McNeill, J. Preparation and encapsulation of highly fluorescent conjugated polymer nanoparticles. *Langmuir* **2006,** *22,* 2956-2960.

For Table of Contents Only